

Dengue epidemics and human mobility

D.H. Barmak, C.O. Dorso, M. Otero, H.G. Solari¹

¹*Departamento de Física, Facultad de Ciencias Exactas y Naturales,
Universidad de Buenos Aires, Pabellón I,
Ciudad Universitaria, Nuñez, 1428,
Buenos Aires, Argentina.*

(Dated: May 8, 2019)

Abstract

In this work we explore the effects of human mobility on the dispersion of a vector borne disease. We combine an already presented stochastic model for dengue with a simple representation of the daily motion of humans on a schematic city of 20x20 blocks with 100 inhabitants in each block. The pattern of motion of the individuals is described in terms of complex networks in which links connect different blocks and the link length distribution is in accordance with recent findings on human mobility. It is shown that human mobility can turn out to be the main driving force of the disease dispersal.

PACS numbers: 87.10.Mn, 87.23.Ge, 05.10.Gg

I. INTRODUCTION

Dengue fever is a vector borne disease produced by a *flavivirus* of the family *flaviviridae* [1]. The main vectors of dengue are *Aedes aegypti* and *Aedes albopictus*.

Dengue fever epidemics have been known for more than two centuries as benign fever epidemics appearing at intervals of one to several decades. Recently the number of countries affected by this epidemic has increased and severe forms have become more frequent.

The research aimed at producing dengue models for public policy use began with Newton and Reiter [2] who introduced a minimal model for dengue in the form of a set of Ordinary Differential Equations (ODE) for the human population disaggregated in Susceptible, Exposed, Infected and Recovered compartments. The mosquitoes population was not modeled in this early work. A different starting point was taken by Focks et al. [3, 4] that began by describing mosquitoes populations in a computer framework named Dynamic Table Model where later the human population (as well as the disease) was introduced [5].

Newton and Reiter's model (**NR**) favors economy of resources and mathematical accessibility, in contrast, Fock's model emphasize realism, these models represent in Dengue two contrasting compromises in the standard trade off in modeling. A third starting point has been recently added. Otero and Solari (**OS**) developed a dengue model [6] which includes the evolution of the mosquitoes population [7, 8] and is spatially explicit. This last model is somewhat in between Fock's and NR as it is formulated as a state-dependent Poisson model with exponentially distributed times.

ODE models have received most of the attention. Some of the works explore: variability of vector population [9], human population [10], the effects of hypothetical vertical transmission of Dengue in vectors [11], seasonality [12], age structure [13] as well as incomplete gamma distributions for the incubation and infectious times [14]. Comparison with real epidemics has shown that there is a need to consider the spatial heterogeneity as well [15].

In a previous work [16] we have developed a dengue model which includes the evolution of the mosquitoes population and is spatially explicit. In that work the spatial spread of the infection was driven by the flights of the mosquitoes that gave rise to a diffusion process. In it we analyzed the evolution of dengue infection in a city of 20X20 blocks with 100 individuals in each one, this population was fixed throughout the calculation and no mobility of the individuals was allowed.

As such, in that model, the spatial evolution of the dengue infection was only driven by the flight of mosquitoes as the mobility of humans was not included. It is usually recognized that human mobility is not only necessary to be included in human infection spread models, but that it might be the main source of the dynamics behind spatiotemporal phenomena on geographic scales (i.e the spread of infection from city to city due to people flying long distances by plane). It is thus very important to address the problem of the mobility of humans and incorporate it into the models to be able to make more reliable predictions, and then, to be able to propose effective public policies against the dispersal of a known or emerging disease.

Including the mobility of the human population in a model is not an easy task given the complexity of human behavior. The first problem to address is the technical and ethical difficulties that arise when trying to get information about the mobility of humans. There are many databases from which this data could be inferred, such as the ones associated to cellular phone networks, credit cards, hotel reservations, flight reservation databases, etc. But as almost all of them are private, most researchers do not have access to them. Moreover, even if we did have them, mixing this diversified information together to get a human mobility model is a hard task by itself. Aside from this particular difficulties, there is an intrinsic bias on the databases if we are going to use them for diseases spread, because its reasonable to think that human behavior will change, or adapt in presence of social awareness of a disease [17–26], and the inferences made on this databases can not take that into account. Moreover there can be a social bias because not everyone may use credit cards, go to hotels, etc.

Whether it is necessary to have a detailed information on the movements of each individual to build up a model, or if it is only needed a coarse grain statistics of the mobility as a whole is an open question wich still has to be answered [27].

Several works tackle the issue of the correct description of the human beings mobility, relaying on different methods and databases [28–35].

As most works focusing on this topic analyze the effect of the human mobility in human-human transmitted diseases [19, 20, 22–26, 36–38], but not in vector borne ones [27, 39, 40], in the present work we show a variation of our previous dengue model which not only includes the flight of the mosquitoes but also the mobility of the humans beings. We then show the

key differences in the results between both our models and conclude on the actual impact of the human behavior on dengue.

In section II we describe the characteristics of the epidemiological model we use in this work encompassing the dynamics of the virus for humans, mosquitoes and the dispersal dynamics for each. In section III we present the results of our numerical investigations which include the analysis of the size and time evolution of the epidemics, the morphological properties of the patterns of spatial distributions of the infections for different mobility patterns and for different densities of mosquitoes. Finally conclusions are drawn in section IV

II. THE EPIDEMIOLOGICAL MODEL

There are four ingredients in this model, the epidemiological dynamics of the infected mosquitoes, the epidemiological dynamics of the infected humans and the mobility pattern of the individuals and mosquitoes. Each of this elements will be discussed in what follows

A. Mosquitoes

The dengue virus does not make any effect to the vector, as such, *Aedes aegypti* populations are independent of the presence of the virus. In the present model mosquitoes populations are produced by the *Aedes aegypti* model [8] with spatial resolution of one block using climatic data tuned to Buenos Aires, a temperate city where dengue circulated in the summer season 2008-2009 [41]. The urbanistic unit of the city is the block, approximately a square of (100m x 100m). Because of the temperate climate the houses are not open as it is often the case in tropical areas. Mosquitoes develop in the center of the block which often presents vegetation and communicates the houses of the block. The model then assumes that mosquitoes belong to the block and not to the houses and they blood-feed with equal probability in any human resident in the block. *Aedes aegypti* is assumed to disperse seeking for places to lay eggs. The mosquitoes population, number of bites per day, dispersal flights and adult mortality information per block is obtained from the mosquitoes model [8].

The time step of the model has been fixed at one day.

The virus enters the mosquito when it bites a viremic human with a probability $p_{hm}(j)$ depending of the day j in the infectious cycle of the human bitten. The cycle continues with the reproduction of the virus within the mosquito (extrinsic period) that lasts τ_m days. After this reproduction period the mosquito becomes infectious and transmits the virus when it bites with a probability p_{mh} . The mosquito follows a cycle Susceptible, Exposed, Infected (SEI) and does not recover. Eventually mosquitoes die with a daily mortality of 0.09 [7]. The adult female mosquitoes population as produced by the *Aedes aegypti* simulation is then split into susceptible, τ_m stages of exposed and one infective compartment according to their interaction with the viremic human population and the number of days elapsed since acquiring the virus.

The mosquito population of each block is not fixed, but instead mosquitoes move around in terms of a simple diffusion process.

B. Humans

The evolution of the disease in one individual human, h , evolves as follows:

Day

$d = d_0$ \rightarrow The virus is transmitted by the bite
of an infected mosquito.

The human enters the exposed stage

$d = d_0 + \tau_E(h)$ \rightarrow The human h enters the infective stage

The human is infective and

$d = d_0 + \tau_E(h) + j$ \rightarrow transmits the virus to a biting mosquito
with probability $p_{hm}(j)$

$d > d_0 + \tau_E(h) + \tau_i$ \rightarrow The human enters the recovered stage.
No longer transmits dengue

In the table above $\tau_E(h)$ stands for the intrinsic incubation time, and τ_i is the viremic time

of each individual. The cycle in the human being is then of the form Susceptible, Exposed, Infected, Recovered (SEIR). Each human has its own value of τ_E which is assigned according to the Nishiura's experimental distribution [42].

As mentioned above, our analysis of the time evolution of dengue fever is performed on a schematic city in which the basic unit is the block and in each block a human population of 100 individuals is placed. An exposed human(index case) is introduced near the center of the grid, on January 1st.

The human population of each block is not fixed in the present work. In order to describe the patterns of mobility of the humans we have adopted the following schematic model. 50% of the population of each block is randomly selected to be mobile, while the other 50% is considered to remain in its original block during the whole analysis. Each mobile individual is assumed to stay 2/3 of the day in its original block, while the other 1/3 of the day she/he will stay in a randomly assigned block according to the corresponding distribution. Each of the mobile individuals is assigned in each case a fixed destination to which it returns everyday. At the end of the day individuals return to their original block. This random assignment is performed according to certain rules that will characterize the mobility pattern. Following recent works on human mobility, referred in the introduction, we require that the movement of each individual a) should be highly predictable [43] and b) the distribution of the lengths of the displacements of the human should follow a truncated Levy distribution [29] which reads:

$$P(r) \propto (r + r_0)^{-\beta} \exp(-r/\kappa). \quad (1)$$

Being $P(r)$ the probability of a human traveling a distance, where r_0 , β and κ are parameters that characterize the distribution. In this work we have used the parameters described in Table I.

TABLE I: Levy-Flight distribution parameters.

	$r_0(m)$	β	κ (m)
1	100	1.65	1500
2	100	2.	1500
3	100	3.	1500
4	100	4.	1500

Such a pattern of mobility of the humans is accomplished by building a network with 50 links starting in each block. The length of the link is distributed according to the proposed length distribution and the final block is chosen at random from those which can be reached by the link. Each link is assigned to a mobile human at the start of the simulation. The distribution of jumps sizes for each type of underlying network is shown on Fig 1.

In order to have reference mobility networks we have also analyzed the case in which the endpoints of the links are completely random. We have also investigated the case in which only one individual per block performs a random jump while the rest of the mobile individuals in the block visit only their neighboring blocks (*Move400*).

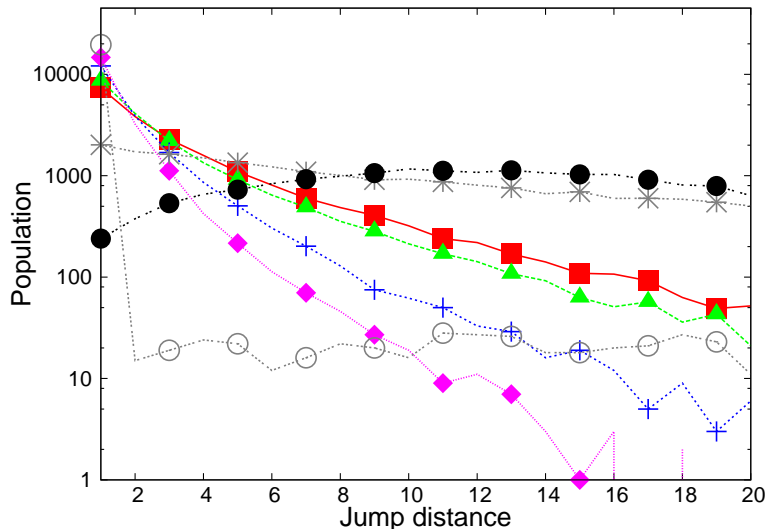


FIG. 1: Distribution of jump length for different mobility patterns. Random(Full circles), Move400(Empty circles), Levy-Flights with $\beta = 1.65$ (Full squares), $\beta = 2$ (Full triangles), $\beta = 3$ (Crosses), $\beta = 4$ (Full diamonds). As comparison, with asterisk is shown the Levy-Flight with parameters from the Barabasi distribution [29].

Once the set of parameters is fixed, different underlying networks are generated and a set of evolutions (typically a couple of thousand events) is performed for such arrangements.

C. The networks

The networks built according to the above mentioned prescription can be analyzed in order to unveil their "small world properties". We have found it interesting to study the

geodesic path i.e. the average minimum path between all the cells.

$$l = \frac{1}{n(n-1)} \sum_{i,j \neq i} d_{ij} \quad (2)$$

with d_{ij} the minimum path between cells i and j , and n the total number of nodes. The minimum path is defined as the minimum number of links that are to be traversed in order to travel from the original block to the destiny block. Therefore, we see that it is a simple average over all the possible pairs of blocks in the system of the minimum distance between each pair.

Another interesting magnitude to explore the characteristics of a network is the so called Clusterization. One of the usual definitions of this magnitude is:

Given a node i with k_i nearest neighbors we define c_i as

$$c_i = \frac{2}{k_i(k_i - 1)} \text{ (number of links between nearest neighbors)} \quad (3)$$

$$C = \frac{1}{n} \sum_i c_i \quad (4)$$

In Table II we show the results of such a calculation.

TABLE II: Clusterization and Mean shortest path for the human mobility networks.

<i>Network</i>	<i>l</i>	<i>C</i>
Random	1.779	0.220
Levy($\beta = 1.65$)	2.006	0.286
Levy($\beta = 2$)	2.112	0.303
Levy($\beta = 3$)	2.532	0.349
Levy($\beta = 4$)	3.092	0.380
Only 400 move	3.884	0.014

We can see from table I that the mean shortest path attains a minimum for the completely random pattern of links and grows as this pattern is replaced by the ones generated by the levy flights. We see that the broader the Levy-Flight is the larger is the average minimum path, as expected.

III. NUMERICAL CALCULATIONS

We have implemented the above described method (The algorithm without human mobility has been fully described in [16]) and have performed extensive calculations for different initial conditions.

The conditions are : mosquitoes breeding sites density, different realizations of the underlying mobility networks and different seasonal conditions.

The number of breeding sites per block explored in this calculations are 50, 100,200,300 and 400. Larger number of breeding sites are considered to be too unrealistic for the system we have in mind i.e. the city of Buenos Aires. Moreover larger number of breeding sites do not add new information to our calculations.

Another relevant condition that we have explored is the underlying mobility network. For each value of the breeding sites density, evolutions with different underlying networks were performed.

Finally we have considered two different seasonal conditions, on Fig. 2 we show the population(top) and temperature(bottom) profiles. In the season-less situation, the temperature remains fixed all along the evolution at $23^{\circ}C$. In this case the mosquito population remains basically constant all along the evolution. In such a case the size of the epidemics is determined by the dynamics of the infection itself subject to the above mentioned boundary conditions. If we adopt the average temperature time-distribution of BA (see figure for details) the population of mosquitoes is a strongly time dependent one, the size of the epidemics might then be severely constrained.

In what follows we will focus on certain properties of the epidemic system that are relevant for the understanding of the characteristics of the time evolution. In first place we study the morphology of the evolving spatial structure of the epidemics. Then we study the final size and time span of the epidemics. Then we include the results of the analysis of a system in which the temperature is kept fixed at 23 degrees Celsius. Finally we study a new magnitude that we name the *power* of the epidemics.

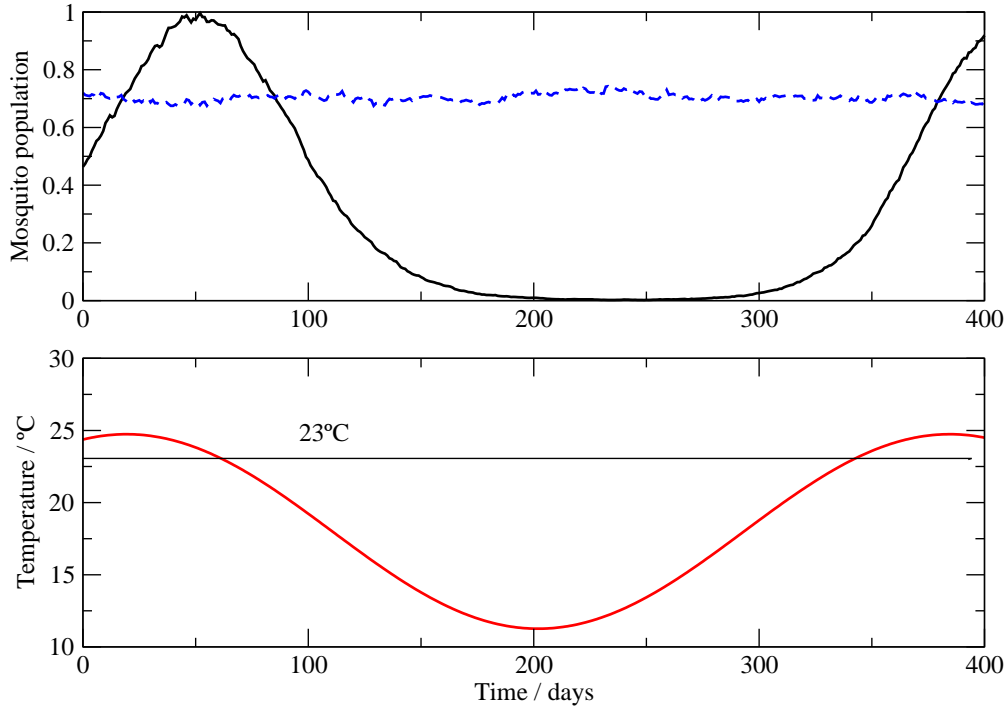


FIG. 2: Top: Normalized mosquitoes population for constant temperature(Dashed) and seasonal variation(full). Bottom: Temperature profile for constant and seasonal variation. Day 0 is set at 1st of January.

A. Morphology of the spatial structure of the epidemics

It is expected that human mobility increases the size and speed of the epidemics.

This happens because each jump (shortcut) when executed by a virus carrying individual may induce the contagion of mosquitoes at the destination block and then generates a new dispersal center for the illness.

In Fig 3 we show the density of recovered individuals at three relevant times for the case in which the dispersal of dengue is driven by the diffusion of mosquitoes only. It is seen that the population of recovered individuals displays a symmetrical pattern as expected from a simple diffusion process.

On the contrary as seen in Fig 4 the pattern for the case in which the human jumps

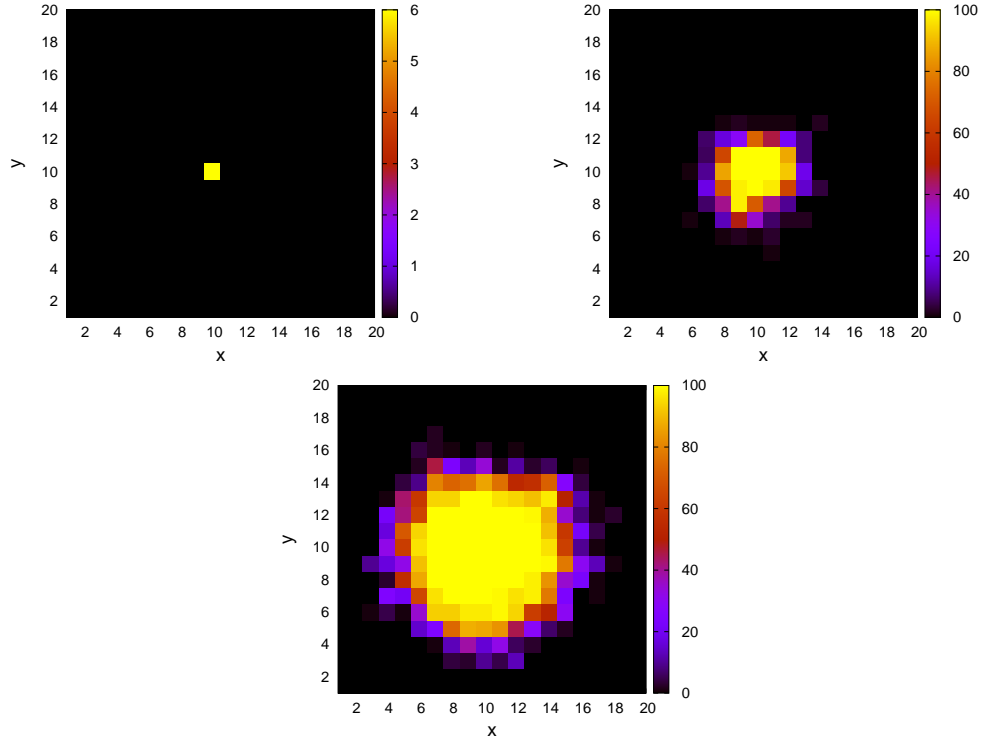


FIG. 3: Spatial distribution of the number of recovered individuals for three times namely 25 days, 81 days and 173 days for the case of a dengue epidemic driven only by the dispersal of mosquitoes. It can be seen that the pattern corresponds to a diffusive process and the evolution is highly symmetric.

follow a Levy-Flight distribution is quite heterogeneous and it can be clearly seen that there is more than one dispersal center.

This observations can be made more quantitative if we calculate the radial correlation function defined as the probability of finding at least one infected (recovered) individual (calculated at the time at which all individuals have returned home) at a block such that it can be reached by a jump of length r from the place at which the initial infected individual one was located (which in this case is a block close to the center of the city).

In what follows we show the result of calculating the radial correlation function for three typical cases namely for the mosquito driven evolution, for the case Levy-Flight with $\beta = 3$ and the case in which only one of the mobile individuals performs random jumps.

From Figs. 5,6,7 is clearly seen that in the presence of human mobility nearly all of the city can be reached by the epidemic in short times. On the one hand the case of mosquitoes

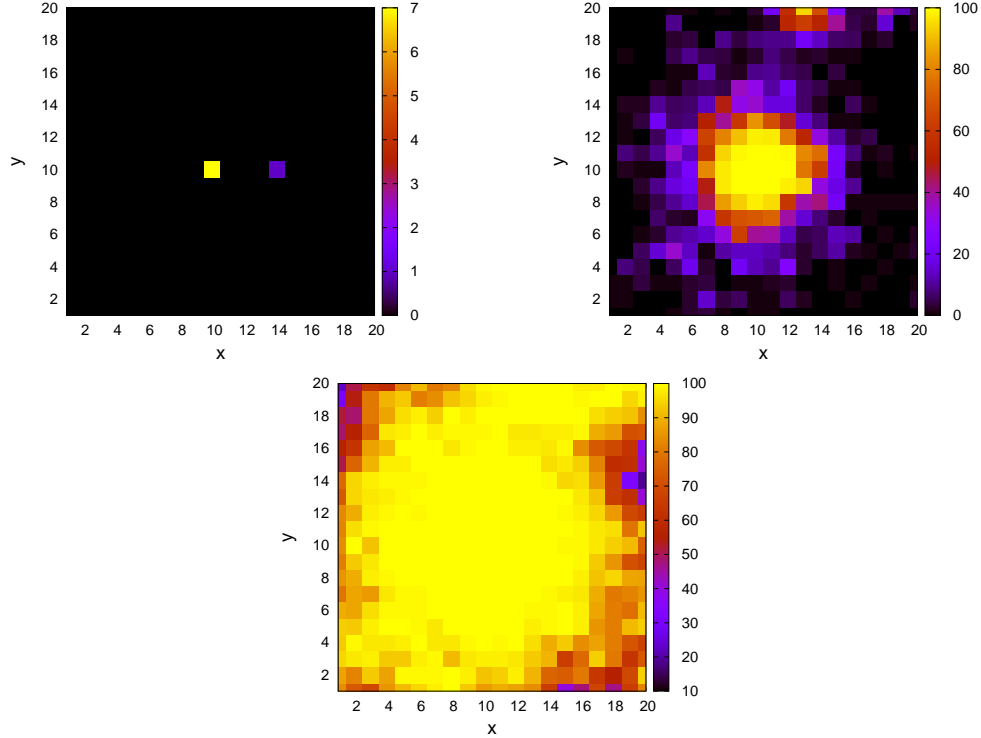


FIG. 4: For the same times as in Fig. 3, the spatial distribution of recovered individuals when their mobility is modeled by a Truncated Levy-Flight with $(\beta) = 3$. It can be seen that, at variance with Fig. 3 the pattern is asymmetrical, moreover the evolution is faster and it can be seen that at $t = 81$ days a second focus is present.

only as driving force the correlation function displays patterns expected for a traveling wavefront. In the other cases the wavefront breaks early in the evolution and the correlation function is different from zero almost everywhere after a few days.

As we have seen in Fig.3) and 4) the structure of the spatial density of, say, humans in state R is highly symmetric and compact for the case without human mobility. As human mobility (of the kind considered in this work) is incorporated both the symmetry and the compactness are lost. In order to explore this behavior in a more quantitative way we define cluster of recovered individuals in the following way. Given a block i we will call it an occupied block if at least one member of its original population is in the recovered state. A cluster (of size larger than one) is a set of occupied blocks in which all constituents have at least a nearest or second nearest neighbor which belongs to the cluster. Then the block i will belong to the cluster if the following relation is satisfied:

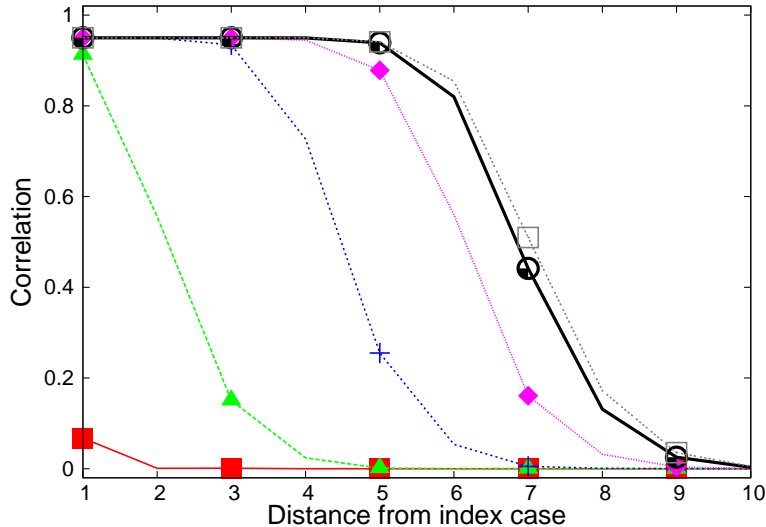


FIG. 5: Radial correlation function as defined in the text for the case in which the spatial evolution of the epidemics is driven by the dispersal of mosquitoes only. Full squares (red) $t = 25days$, full triangles (green) $t = 57days$, crosses (blue) $t = 89days$, diamond (violet) $t = 121days$ open circles (black) $t = 153days$, open squares (gray) $t = 189days$. The pattern of variation is quite regular as expected for a diffusive case.

$$i \in C \iff \exists j \in C / i \text{ is neighbor of } j \quad (5)$$

We define the mass of a cluster as the number of recovered individuals in the cluster.

The results are displayed in the Fig 8.

It can be seen that for the case of simple diffusion all of the mass is concentrated in the biggest cluster. On the other hand for the random case there is a time (around 50 days into the epidemic) at which only about 65% of the mass is in the biggest cluster. This is due to the emergence of secondary foci generated by infective humans who perform long jumps.

B. Sizes and time span of the epidemics

One of the main observables in this kind of problems is the final size of the epidemics. In what follows we show Figure 9 a comparison of the final size of the epidemics in terms of the boxplots corresponding to different values of the breeding sites density for different patterns of human mobility. As described above we have two limiting situations *a*) the case in which the moving humans perform jumps with completely random destinations and *f*) the case in

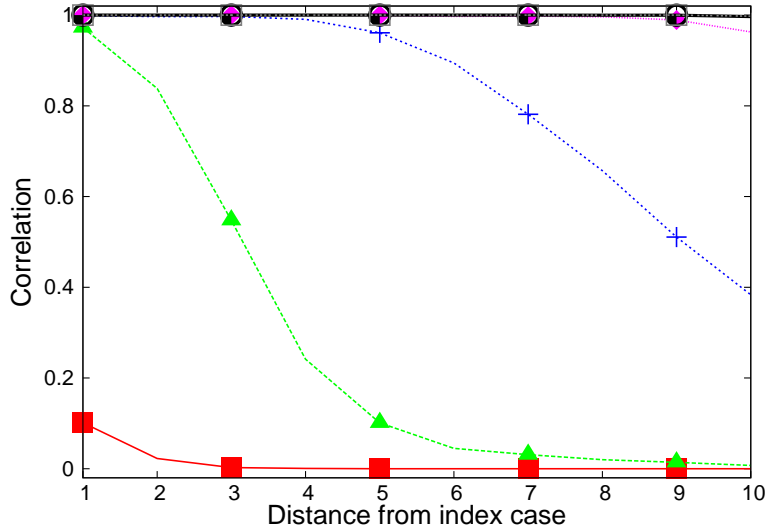


FIG. 6: Radial correlation function as defined in the text for the case in which the humans move with the Levy-Flight($\beta = 3$) distribution. Full squares (red) $t = 25days$, full triangles (green) $t = 57days$, crosses (blue) $t = 89days$, diamond (violet) $t = 121days$ open circles(black) $t = 153days$, open squares (gray) $t = 189days$.

which the dispersal of the epidemics is only due to the diffusion of mosquitoes. In between we have the patterns related to the length of the jump given by a truncated Levy-Flight characterized by the different set of parameters shown in table I i.e. $\beta = 1.65, 2, 3$ and 4 (keep in mind the smaller β the closer to the random case). The corresponding results are displayed in panels $b - e$.

Finally in Fig. 10 we show (left panel) the case in which only one of the mobile humans in each block performs a jump to a random destination while the others move to nearest neighbors. For the sake of completeness we show on the right panel the boxplot corresponding to the mosquito only driven evolution.

It is immediate to see that the effect of human mobility for all the cases is to increase the final size of the epidemics with respect to the case in which the mosquitoes diffusion is the only driving force. Moreover in the case of completely random mobility and for the Levy-Flight with $\beta = 1.65$ we get that for the highest BS density proposed in this work, the epidemics spreads over the whole population.

Figure 11 shows the duration distribution of the epidemics as a function of the different patterns of human mobility and for two constant breeding site densities of 200 BS/ha (Top) and 400 BS/ha (Bottom) respectively. For 200 BS (Top) all boxplots present a similar

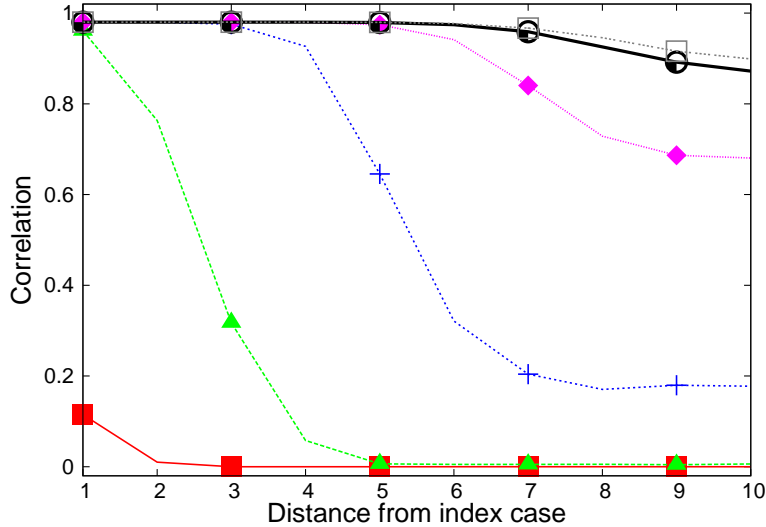


FIG. 7: Radial correlation function as defined in the text for the case in which only one human per block moves at random, and the rest move to neighboring blocks. Full squares (red) $t = 25$ days, full triangles (green) $t = 57$ days, crosses (blue) $t = 89$ days, diamond (violet) $t = 121$ days, open circles (black) $t = 153$ days, open squares (gray) $t = 189$ days.

spread of data but a slight tendency of increase of the median from left to right (from the case without mobility to the complete random pattern). Instead, for 400 BS the tendency is to decrease from left to right. (This behavior will be properly discussed in terms of the Power of the epidemics, see below)

C. Behavior of the model at constant temperature

Figure 12 shows the duration distribution of the epidemics as a function of the different patterns of human mobility for a constant breeding site density of 400 BS/ha and a constant temperature of 23 degrees Celsius. We see that the maximum duration of the epidemic takes place for the case of no human mobility and it shortens as the patterns of mobility of the individuals tend to the completely random one. It is also interesting to note that in this case the epidemics involves the whole population.

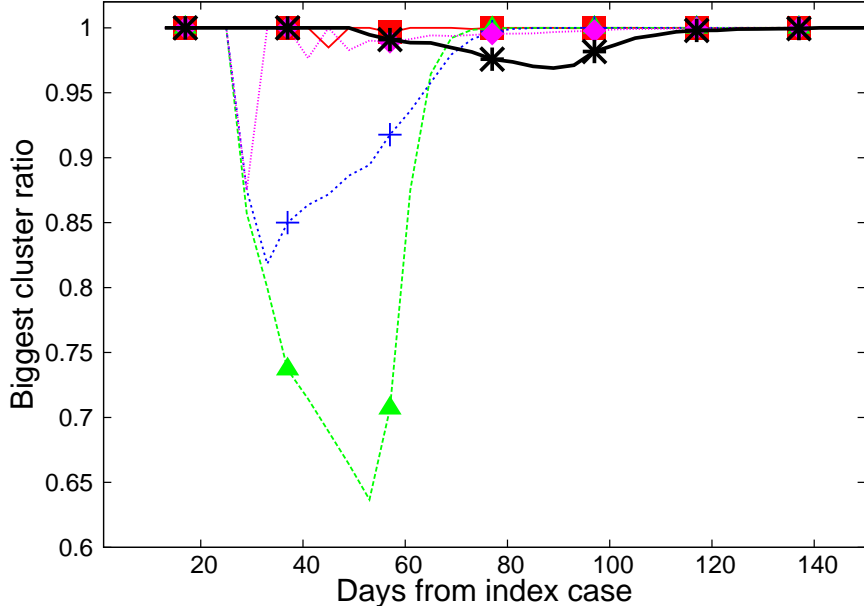


FIG. 8: Ratio between the size of the biggest cluster (in terms of the number of recovered humans) and the total number of recovered. Diffusive (Red full squares), random (Green full triangles), Levy-Flight($\beta = 1.65$) (blue crosses), Levy-Flight($\beta = 4$) (violet full diamonds), Move400 (Black asterisks).

D. Power of the epidemic

We define the mean power of the epidemic as the ratio between the median of the final size of the epidemic and the median of the duration of the epidemics.

$$P_m = \frac{S}{\tau} \quad (6)$$

Figure 13 shows the mean power for three conditions: (a) 400 BS and constant temperature of 23 degrees, (b) 400 BS and seasonal variation of temperature and (c) 200 BS and seasonal variation of temperature. The P_m grows with broader jump length distributions and with higher BS densities. For the case of 400 BS is higher for constant temperature than for seasonal variation of temperature. If we compare 400 BS and 200 BS (for seasonal variation of temperature) we see the same increasing tendency of P_m with human mobility but this value is higher for 400 BS than for 200 BS. (For the case of 400 BS and constant T the increase of the power of the epidemic is a consequence of the reduction of its duration as the pattern of human mobility approaches the fully random case. At constant T all of

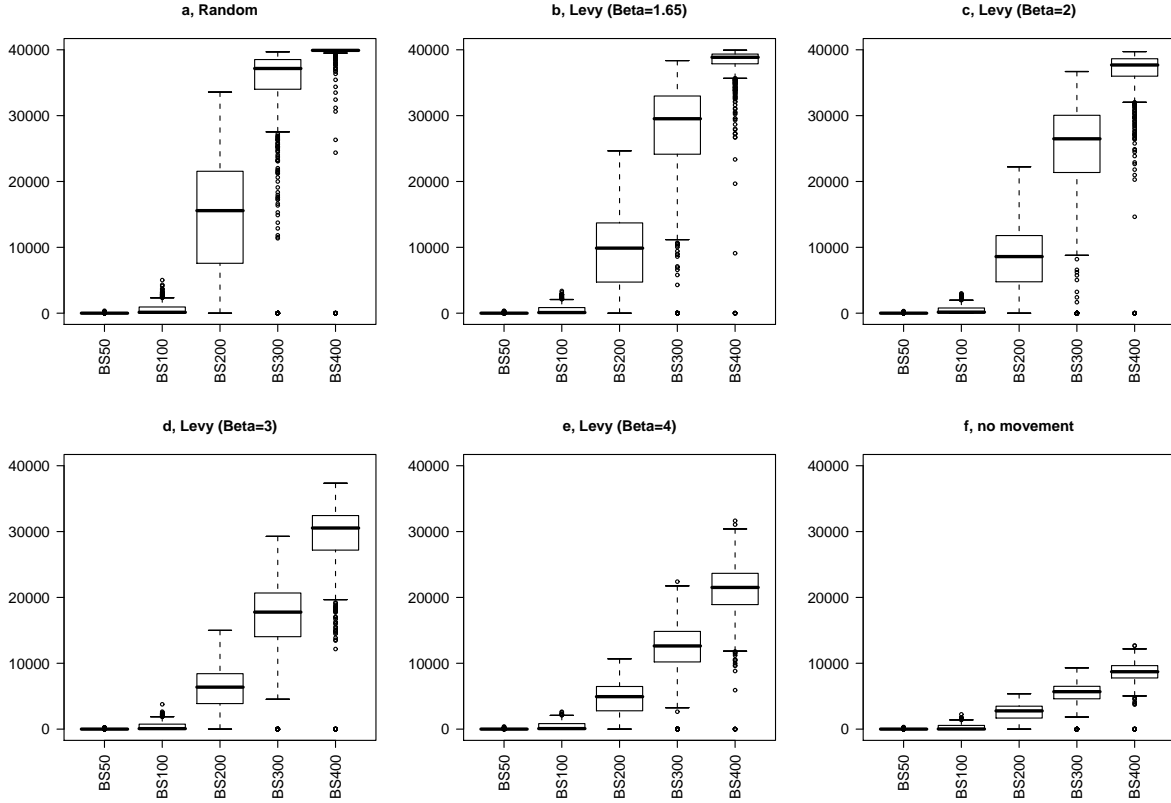


FIG. 9: Boxplots graphs of the epidemic size for different patterns of human mobility: (a) random, (b) $\text{levy}(\beta=1.65)$, (c) $\text{levy}(\beta=2)$, (d) $\text{levy}(\beta=3)$, (e) $\text{levy}(\beta=4)$ and (f) move400.

the population gets infected. On the other hand, when the Temperature is not fixed it severely constrains the mosquitoes population and then the increase in P_m is mainly due to the increase of the size of the infected population as the time span of the epidemics is only mildly dependent on the driving force of the dispersal.

IV. CONCLUSIONS

In this work we have explored the effect of human mobility on the dynamics of a vector borne infection. We have added this characteristic of human behavior on an already tested model of dengue dispersal when the dynamics is driven by mosquitoes alone. We have analyzed the case of a schematic city of 20x20 blocks with 100 individuals per block.

We have considered two temperature profiles, on the one hand a simple constant temperature one and a realistic time distribution corresponding to the city of Buenos Aires, Argentina.

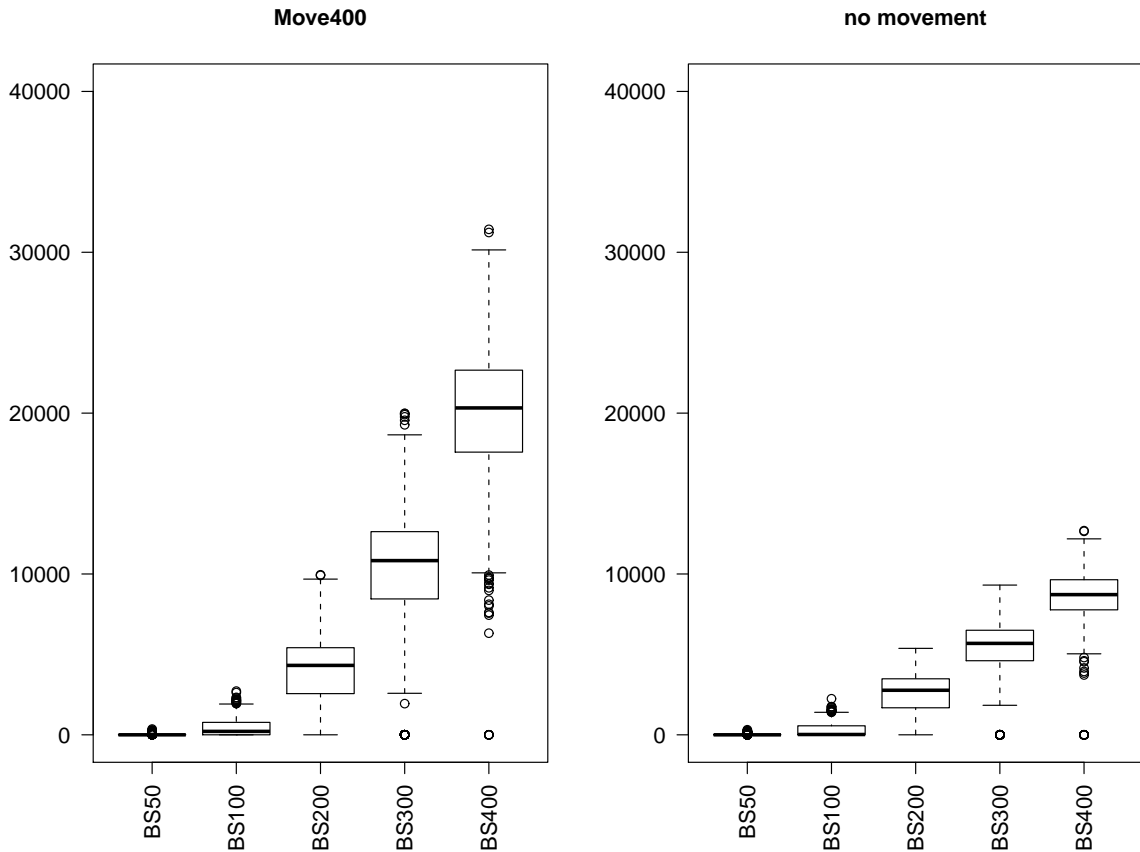


FIG. 10: Boxplots graphs of the epidemic size for different patterns of human mobility: (Left) move400 and (Right) no human mobility.

Another variable in our analysis has been the number of breeding cites in the city, we have considered 50,100, 200, 300 and 400 breeding cites per block.

Human mobility has been described by superimposing diverse kinds of networks in which links represent the daily movement of humans. The distribution of lengths of this links are derived from recent studies on human motion and in particular, taking into account the finding that human behavior is highly predictable. We have also considered reference patterns i.e purely random motion and random motion of a single human per block.

We have explored different observables like size and duration of the outbreaks, and complementary the morphological characteristics of the pattern of recovered individuals.

We have found that human mobility strongly enhances the infection dispersal. Even for the case in which just one individual per block can perform a long jump. This effect can be traced to the fact that when the disease dispersal is driven by mosquitoes alone we have a

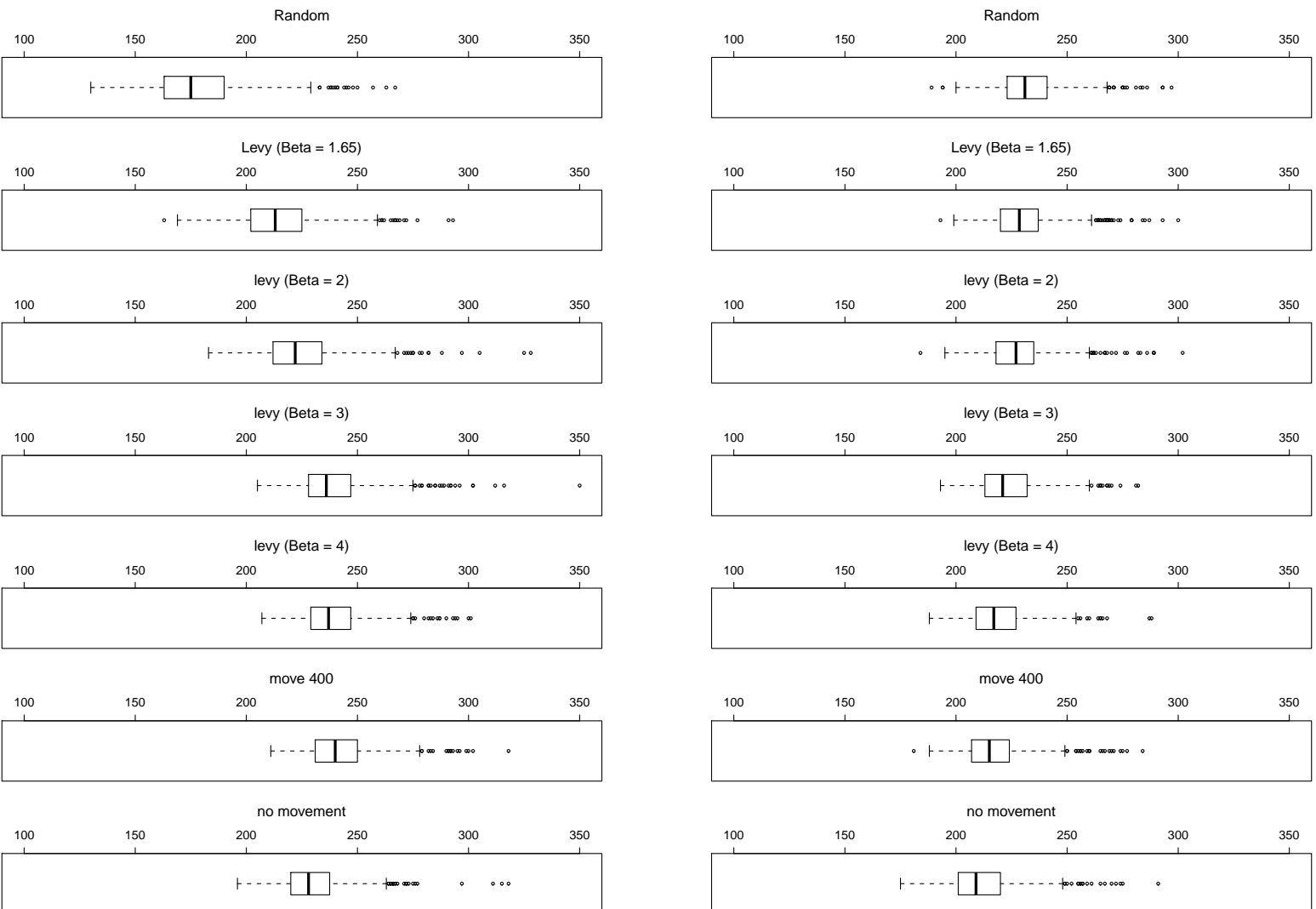


FIG. 11: Comparison of the duration of the epidemic outbreaks for the different patterns of human mobility, 200 breeding sites/ha (Top) and 400 breeding sites/ha (Bottom).

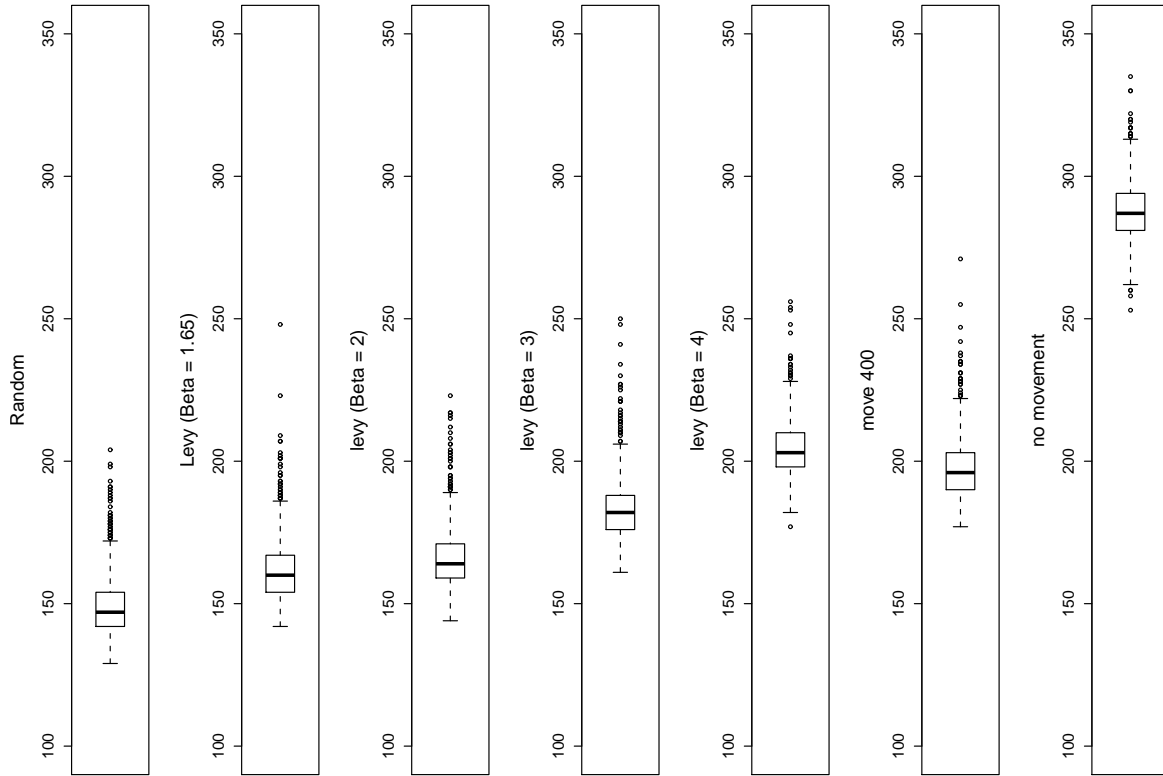


FIG. 12: Comparison of the duration of epidemics for the different patterns of human mobility at a constant temperature of 23 degrees Celsius (400 breeding sites / ha).

single focus that expands due to diffusive kind of dynamics. When human mobility is taken into account, multiple loci appear as the time evolution is followed

Human mobility increases the size and the speed of propagation of the outbreaks. This feature can be captured by the magnitude "Power of the epidemics" defined as the quotient of the size of the epidemics divided by the its time span. This magnitude displays a monotonous increase as the Mean Length Path of the network describing the daily human mobility pattern decreases.

This findings indicate that human mobility might turn out to be the main driving force in the epidemics dynamics.

Both in the case of fixed temperature and seasonal variational one, human motion gives rise to faster and more widespread epidemics.

Finally this findings indicate that, when considering measures to fight epidemics dispersal

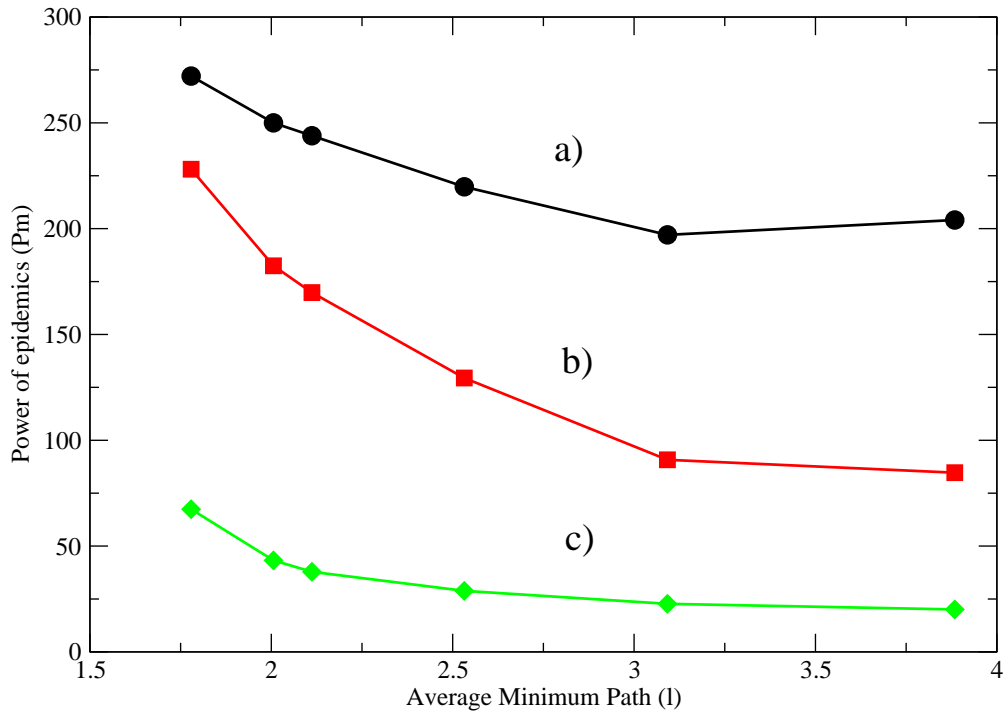


FIG. 13: Comparison of the mean power of the epidemics for the different patterns of human mobility (from left to right: Random, Levy1.65, Levy2, Levy3, Levy4, Move400), characterized by the average minimum path for three conditions: (a) 400 BS and constant temperature of 23 degrees and (b) 400 BS and (c) 200 BS for seasonal variation of temperature.

human motion should be one of the top concerns. We are presently exploring this issue.

Acknowledgments

C.O.D, M.O and H.G.S are members of the Carrera del Investigador CONICET. D.H.B is a fellow of the CONICET. We thank the support by the University of Buenos Aires (grant X210).

-
- [1] D. J. Gubler, *Clinical Microbiology Review* **11**, 480 (1998).
 - [2] E. A. C. Newton and P. Reiter, *Am. J. Trop. Med. Hyg.* **47**, 709 (1992).
 - [3] D. A. Focks, D. C. Haile, E. Daniels, and G. A. Moun, *Journal of Medical Entomology* **30**,

- 1003 (1993).
- [4] D. A. Focks, D. C. Haile, E. Daniels, and G. A. Mount, *Journal of Medical Entomology* **30**, 1019 (1993).
- [5] D. A. Focks, D. C. Haile, E. Daniels, and D. Keesling, *Am. J. Trop. Med. Hyg.* **53**, 489 (1995).
- [6] M. Otero and H. G. Solari, *Mathematical Biosciences* **223**, 32 (2010).
- [7] M. Otero, H. G. Solari, and N. Schweigmann, *Bull. Math. Biol.* **68**, 1945 (2006).
- [8] M. Otero, N. Schweigmann, and H. G. Solari, *Bulletin of Mathematical Biology* **70**, 1297 (2008).
- [9] L. Esteva and C. Vargas, *Mathematical Biosciences* **150**, 131 (1998).
- [10] L. Esteva and C. Vargas, *Journal of Mathematical Biology* **38**, 220 (1999).
- [11] L. Esteva and C. Vargas, *Mathematical Biosciences* **167**, 51 (2000).
- [12] L. M. Bartley, C. A. Donnelly, and G. P. Garnett, *Transactions of the royal society of tropical medicine and hygiene* **96**, 387 (2002).
- [13] P. Pongsumpun and I. M. Tang, *Mathematical and Computer Modelling* **37**, 949 (2003).
- [14] G. Chowella, P. Diaz-Dueas, J. Miller, A. Alcazar-Velazco, J. Hyman, P. Fenimore, and C. Castillo-Chavez, *Mathematical Biosciences* **208**, 571 (2007).
- [15] C. Favier, D. Schmit, C. D. M. Mller-Graf, B. Cazelles, N. Degallier, B. Mondet, and M. A. Dubois, *Proceedings of the Royal Society (London): Biological Sciences* **272**, 1171 (2005).
- [16] M. Otero, D. Barmak, C. Dorso, H. Solari, and M. Natiello (2010), arXiv:1012.1281v1 [q-bio.PE].
- [17] J. M. Epstein, J. Parker, D. Cummings, and R. A. Hammond, *PLoS ONE* **3**, e3955 (2008), URL <http://dx.doi.org/10.1371/journal.pone.0003955>.
- [18] T. Gross and B. Blasius, *J. R. Soc. Interface* **5**, 259 (2008), URL <http://dx.doi.org/10.1098/rsif.2007.1229>.
- [19] T. Gross, C. J. D’Lima, and B. Blasius, *Physical Review Letters* **96**, 208701+ (2006), URL <http://dx.doi.org/10.1103/PhysRevLett.96.208701>.
- [20] S. Risau-Gusmans, , and D. H. Zanette, *Journal of Theoretical Biology* **257**, 52 (2009), ISSN 00225193, URL <http://dx.doi.org/10.1016/j.jtbi.2008.10.027>.
- [21] D. H. Zanette (2007), arXiv e-prints, 0707.1249, URL <http://arxiv.org/abs/0707.1249>.
- [22] D. H. Zanette and S. R. Gusman, *Journal of Biological Physics* **34**, 135 (2007), 0711.0874, URL <http://arxiv.org/abs/0711.0874>.

- [23] W. Lig, Y. Jia-Ren, Z. Jian-Guo, and L. Zi-Ran, Chinese Physics **16**, 2498+ (2007), ISSN 1009-1963, URL <http://dx.doi.org/10.1088/1009-1963/16/9/002>.
- [24] N. H. Fefferman and K. L. Ng, Physical Review E **76**, 031919+ (2007), URL <http://dx.doi.org/10.1103/PhysRevE.76.031919>.
- [25] S. Funk, M. Salathé, and V. A. A. Jansen, Journal of The Royal Society Interface (2010), URL <http://dx.doi.org/10.1098/rsif.2010.0142>.
- [26] Z. Zhao, J. P. Calderón, C. Xu, G. Zao, D. Fenn, D. Sornette, R. Crane, P. M. Hui, and N. F. Johnson, Physical Review E **81**, 056107+ (2010), URL <http://dx.doi.org/10.1103/PhysRevE.81.056107>.
- [27] L. Sattenspiel, *The Geographic Spread of Infectious Diseases: Models and Applications* (Princeton University, 2009).
- [28] I. Rhee, M. Shin, S. Hong, K. Lee, and S. Chong, Technical Report, Computer Science Department, North Carolina State University (2007).
- [29] M. C. Gonzalez, C. A. Hidalgo, and A.-L. Barabasi, Nature **453**, 779 (2008).
- [30] D. Brockmann, L. Hufnagel, and T. Geisel, Nature **439** (2006).
- [31] L. H. D. Brockmann, *The scaling law of human travel - A message from George* (World Scientific, 2007).
- [32] G. Chowell, J. M. Hyman, S. Eubank, and C. Castillo-Chavez, Physical Review E **68**, 661021 (2003).
- [33] C. Cattuto, W. Van den Broeck, A. Barrat, V. Colizza, J.-F. Pinton, and A. Vespignani, PLoS ONE **5**, e11596 (2010), URL <http://dx.doi.org/10.1371/journal.pone.0011596>.
- [34] J. Candia, M. C. Gonzalez, P. Wang, and T. Schoenharl (2007), detection of anomalous local cell pattern, URL <http://arxiv.org/pdf/0710.2939>.
- [35] P. Wang and M. C. Gonzalez, Royal Society of London Philosophical Transactions Series A **367**, 3321 (2009).
- [36] A. Buscarino, L. Fortuna, M. Frasca, and V. Latora, European Physics Letters **82**, 38002 (2008).
- [37] X. Li, L. Cao, and G. F. Cao, The European Physical Journal B - Condensed Matter and Complex Systems (2010), ISSN 1434-6028, URL <http://dx.doi.org/10.1140/epjb/e2010-00090-9>.
- [38] M. Keeling and K. T. Eames, Journal of the Royal Society Interface **22**, 295 (2005), ISSN

- 1742-5689, URL <http://dx.doi.org/10.1098/rsif.2005.0051>.
- [39] P. Pongsumpun, D. G. Lopez, C. Favier, L. Torres, J. Llosa, and M. Dubois, *Tropical Medicine and International Health* **13**, 1180 (2008).
- [40] S. T. Stoddard, A. C. Morrison, G. M. Vazquez-Prokopec, V. P. Soldan, T. J. Kochel, U. Kitron, J. P. Elder, and T. W. Scott, *PLoS Negl Trop Dis* **3**, e481 (2009), URL <http://dx.doi.org/10.1371/journal.pntd.0000481>.
- [41] A. Seijo, Y. Romer, M. Espinosa, J. Monroig, S. Giamperetti, D. Ameri, and L. Antonelli, *Medicina* **69**, 593 (2009), iISSN 0025-7680.
- [42] H. Nishiura and S. B. Halstead, *Journal of Infectious Diseases* **195**, 1007 (2007).
- [43] C. Song, Z. Qu, N. Blumm, and A.-L. Barabasi, *Science* **327**, 1018 (2010), <http://www.sciencemag.org/cgi/reprint/327/5968/1018.pdf>, URL http://www.barabasilab.com/pubs/CCNR-ALB_Publications/201002-19_Science-Predictability/201